

Probing thermal properties of vanadium dioxide thin films by time-domain thermoreflectance without metal film

Qing-Jian Lu(陆青鑑), Min Gao(高敏), Chang Lu(路畅), Fei Long(龙飞), Tai-Song Pan(潘泰松), and Yuan Lin(林媛)
Citation: Chin. Phys. B, 2021, 30 (**9**): 096801. DOI: 10.1088/1674-1056/abea94
Journal homepage: http://cpb.iphy.ac.cn; http://iopscience.iop.org/cpb

What follows is a list of articles you may be interested in

Effect of Mo doping on phase change performance of Sb_2Te_3

Wan-Liang Liu(刘万良), Ying Chen(陈莹), Tao Li(李涛), Zhi-Tang Song(宋志棠), and Liang-Cai Wu(吴良才)
Chin. Phys. B, 2021, 30 (**8**): 086801. DOI: 10.1088/1674-1056/abe22d

Surface effects on the thermal conductivity of silicon nanowires

Hai-Peng Li(李海鹏), Rui-Qin Zhang(张瑞勤)
Chin. Phys. B, 2018, 27 (**3**): 036801. DOI: 10.1088/1674-1056/27/3/036801

Thermoelectric properties of two-dimensional hexagonal indium-VA

Jing-Yun Bi(毕京云), Li-Hong Han(韩利红), Qian Wang(王倩), Li-Yuan Wu(伍力源), Ruge Quhe(屈贺如歌), Peng-Fei Lu(芦鹏飞)
Chin. Phys. B, 2018, 27 (**2**): 026802. DOI: 10.1088/1674-1056/27/2/026802

Effect of isotope doping on phonon thermal conductivity of silicene nanoribbons: A molecular dynamics study

Run-Feng Xu(徐润峰), Kui Han(韩奎), Hai-Peng Li(李海鹏)
Chin. Phys. B, 2018, 27 (**2**): 026801. DOI: 10.1088/1674-1056/27/2/026801

Fabrication of VO_2 thin film by rapid thermal annealing in oxygen atmosphere and its metal-insulator phase transition properties

Liang Ji-Ran, Wu Mai-Jun, Hu Ming, Liu Jian, Zhu Nai-Wei, Xia Xiao-Xu, Chen Hong-Da
Chin. Phys. B, 2014, 23 (**7**): 076801. DOI: 10.1088/1674-1056/23/7/076801

Probing thermal properties of vanadium dioxide thin films by time-domain thermoreflectance without metal film*

Qing-Jian Lu(陆青鑑)[1,2], Min Gao(高敏)[1,2,†], Chang Lu(路畅)[1,2], Fei Long(龙飞)[3], Tai-Song Pan(潘泰松)[1,2], and Yuan Lin(林媛)[1,2,4,‡]

[1] *School of Materials and Energy, University of Electronic Science and Technology of China, Chengdu* 610054, *China*
[2] *State Key Laboratory of Electronic Thin Films and Integrated Devices, University of Electronic Science and Technology of China, Chengdu* 610054, *China*
[3] *Guangxi Key Laboratory of Optical and Electronic Materials and Devices, School of Materials Science and Engineering, Guilin University of Technology, Guilin* 541004, *China*
[4] *Medico-Engineering Cooperation on Applied Medicine Research Center, University of Electronic Science and Technology of China, Chengdu* 610054, *China*

(Received 30 December 2020; revised manuscript received 1 February 2021; accepted manuscript online 1 March 2021)

Vanadium dioxide (VO_2) is a strongly correlated material, and it has become known due to its sharp metal–insulator transition (MIT) near room temperature. Understanding the thermal properties and their change across MIT of VO_2 thin film is important for the applications of this material in various devices. Here, the changes in thermal conductivity of epitaxial and polycrystalline VO_2 thin film across MIT are probed by the time-domain thermoreflectance (TDTR) method. The measurements are performed in a direct way devoid of deposition of any metal thermoreflectance layer on the VO_2 film to attenuate the impact from extra thermal interfaces. It is demonstrated that the method is feasible for the VO_2 films with thickness values larger than 100 nm and beyond the phase transition region. The observed reasonable thermal conductivity change rates across MIT of VO_2 thin films with different crystal qualities are found to be correlated with the electrical conductivity change rate, which is different from the reported behavior of single crystal VO_2 nanowires. The recovery of the relationship between thermal conductivity and electrical conductivity in VO_2 film may be attributed to the increasing elastic electron scattering weight, caused by the defects in the film. This work demonstrates the possibility and limitation of investigating the thermal properties of VO_2 thin films by the TDTR method without depositing any metal thermoreflectance layer.

Keywords: vanadium dioxide thin film, thermal conductivity, time-domain thermoreflectance

PACS: 68.60.Dv, 66.30.Xj **DOI:** 10.1088/1674-1056/abea94

1. Introduction

Vanadium dioxide (VO_2), by virtue of its sharp metal–insulator transition (MIT) near room temperature and the associated dramatic changes in electrical and optical properties, presents promising applications in electrical and optical switches.[1–6] While the predominant research thrust has been oriented to the intensive exploration of its phase transition mechanism and applications in memory devices and other smart devices, the mechanistic exploration of its thermal transport mode has attracted much less attention.[7–12] Only very recently, Sangwook *et al.*[10] and Jin *et al.*[11] have done some researches on the thermal transport mode of VO_2, including the abnormal low electronic thermal conductivity and the non-quasiparticle transport mechanism in the metallic phase, which provides a different perspective to further understand the electron–electron interaction in this strongly correlated material.

Sangwook *et al.*'s work focused on single-crystal VO_2 nanowire, but VO_2 thin films were technically more useful in the predicted devices. In this study, we use the time-domain thermoreflectance (TDTR) method[13–17] to investigate the cross-plane thermal properties of VO_2 thin films. The TDTR has been demonstrated to be a powerful method to investigate the thermal properties of thin films and multilayered films.[18–21] Unlike the most widely used 3ω method in measuring the thermal properties of films, TDTR allows detecting the thermal properties of electrically conducting or semiconducting materials. In practical, most TDTR experiments require a thin metal layer (Pt, Au, Mo or Al) as a thermoreflectance layer in probing the surface temperature changes because the reflectivity of metal layer changes linearly with temperature. Some previous work utilized the TDTR to investigate the cross-plane thermal properties of VO_2 films by depositing a metal layer on the top of the film.[7,8] However, the interfacial thermal resistance between the metal layer and the specimen was difficult to eliminate, which might cause additional measurement uncertainties. On the other hand, the

*Project supported by the National Natural Science Foundation of China (Grant Nos. 61825102, 51872038, and 52021001) and the "111" Project, China (Grant No. B18011).

†Corresponding author. E-mail: mingao@uestc.edu.cn
‡Corresponding author. E-mail: linyuan@uestc.edu.cn

© 2021 Chinese Physical Society and IOP Publishing Ltd

reflectivity and transmittance of VO_2 film change with temperature, which is similar to those of the metallic thermoreflectance layer, suggesting the possibility of measuring the thermal transport properties of VO_2 film by using TDTR without depositing any metal layer on the film.

In this study, we fabricate VO_2 thin films on the Al_2O_3(10-10) substrate and fluorine mica substrate, respectively. The VO_2 thin film epitaxially grown on the Al_2O_3 substrate exhibits high crystalline quality and bonds well with the substrate. The fluorine mica substrate is a van de Waals (vdW) substrate, which means a weak effect on the in-plane growth direction of the as-grown film. By measuring the TDTR spectra of the VO_2 films on these two different substrates below and above the phase transition temperature through using the TDTR method without depositing any metal layer on the films, we observe the reasonable thermal conductivities of VO_2 thin films when the thickness values of the films are greater than 100 nm. Meanwhile, by comparing the thermal conductivity changes of VO_2 films on different substrates across the MIT, we find that it is correlated with the electrical conductivity change rate. Our results show that the TDTR method can be feasible in investigating the thermal transport properties of VO_2 films without depositing any metal thermoreflectance layer. Meanwhile, the limitation of this method will also be discussed.

2. Experiment

The VO_2 thin films were grown on Al_2O_3(10-10) substrate and fluorine mica substrate by using a polymer-assisted deposition (PAD) technique.[22–24] First, the polymer solution was prepared by dissolving 2.0-g polyethyleneimine (PEI, Mw≈10000), 2.0-g ethylenediamine tetra acetic acid (EDTA) and 0.8-g ammonium metavanadate (NH_4VO_3) in 60-mL deionized (DI) water. Then the solution was filtered in an ultrafiltration device (Amicon 8050) to obtain a precursor solution containing 20.5-mg V ions per mL as measured by inductively coupled plasma optical emission spectrometer (ICP-OES). The as-prepared precursor solution was spin-coated on the Al_2O_3(10-10) and fluorine mica substrates at a rate of 6500 rpm for 40 s, respectively. Finally, the precursor films were annealed at 505 °C in forming gas (H_2 = 1.5% and N_2 = 98.5%) for 2 h. The spin-coating and annealing process was repeated to obtain VO_2 thin films of various thickness values. A detailed description of the synthesis process can be found in previous literature.[23,24] The VO_2 thin films of four different thickness values were grown on the Al_2O_3 substrates and the fluorine mica substrates. Using scanning electron microscopy, the thickness values were determined to be about 30 nm, 60 nm, 110 nm, and 150 nm, respectively.

The thermal conductivity of the VO_2 thin film was measured by a nanosecond pulse laser thermal reflector system (Nano TR, PicoTherm, Japan). The experimental set-up is schematically shown in Fig. 1. A ceramic heating plate, controlled by a direct current (DC) power, was used to heat the samples and the temperature of the ceramic heating plate was detected by a thermocouple thermometer. A 1550-nm pulsed laser with pulse width of 1 ns and energy of 100 mW was used to heat the sample and a 785-nm continuous wave laser was used to probe the variation of temperature of the sample with time. A lock-in amplifier in this system was used to measure a small change of temperature with time.

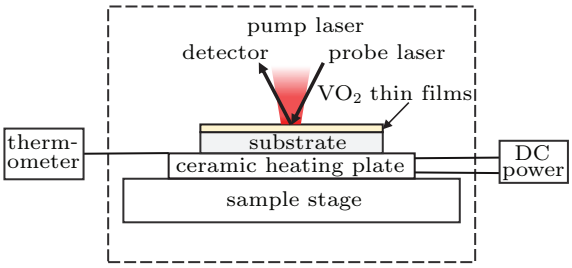


Fig. 1. Schematic set-up of nanosecond pulse laser thermal reflection system.

The crystal quality of the VO_2 thin films was examined by a high-resolution x-ray diffractometer (HR-XRD, Bruker D8 Advance). The variation of the resistance of the thin films with temperature was measured by B2902A (Keysight), while the temperatures of the samples were controlled by LakeSore 325 during the measurements.

3. Results and discussion

The crystal structures of the VO_2 thin films on the fluorine mica and Al_2O_3(10-10) substrates are investigated by XRD θ–2θ scans as shown in Fig. 2. For the VO_2 thin films on the Al_2O_3 substrates, only the x-ray diffraction peak of $VO_2(-402)$ is observed besides the peaks from the substrates. Additionally, our previous Φ-scan confirmed the epitaxial growth of VO_2 on Al_2O_3(10-10) substrate.[24] For the VO_2 thin films on the fluorine mica substrates, the x-ray diffraction peaks of VO_2(011) and VO_2(022) are detected besides the peaks from the substrates as shown in Fig. 2, suggesting the growth mode with a highly preferred crystalline orientation. However, the Φ-scan does not detect the diffraction peak of VO_2, which is possibly due to the disordered in-plane crystalline alignment.

The TDTR is employed to measure the thermal conductivity of the VO_2 thin film. First, we measure the thermal reflectance curves of 60-nm-thick VO_2 thin films coated with two kinds of 100-nm-thick metal films (Pt film and Mo film) as shown in Fig. S1 in the supplementary materials. The large difference between the observed two thermal reflectance curves indicates that the interface thermal resistance between the metal film and the sample should be carefully controlled to

reduce the interface effect. To explore the methods of measuring TDTR without depositing the metallic thermoreflectance layer, we first check the change of the reflectivity of VO_2 film with temperature. As demonstrated by the measurements with a 785-nm laser, the reflectivity of 150-nm-thick VO_2 film exhibits an approximately linear relationship with temperature in both the insulating state and the metallic state as shown in Fig. S2 in the supplementary materials. This implies that the thermal reflectance curve of VO_2 film can be obtained through the TDTR method without depositing an extra metal thermoreflectance layer on the top. However, in the phase transition process, the reflectivity of vanadium dioxide film displays sharp changes, which in turn can present abnormal thermal reflectance curves in TDTR. It should be noted that by measuring the temperature dependent reflectivity of the VO_2 film coated with 100-nm Pt film (shown in Fig. S3 in the supplementary materials), we find that it also exhibits a sharp change in the phase transition process, thereby confirming that the abnormal reflected signals of the VO_2 film cannot be completely screened even by the 100-nm-thick Pt film. Therefore, we can analyze only the thermal reflectance curves of VO_2 films beyond the phase transition region by using this method.

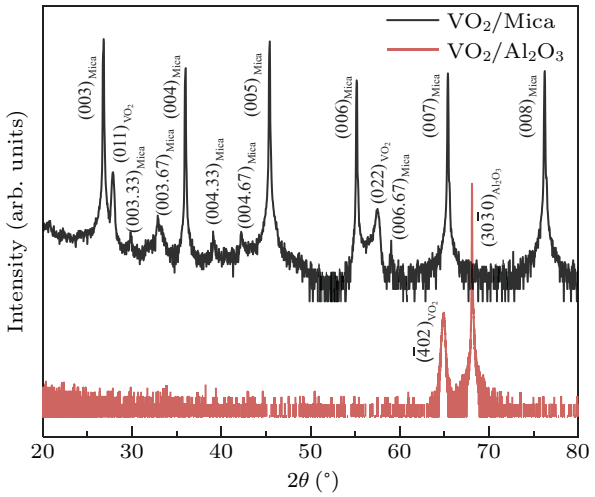


Fig. 2. X-ray diffraction of VO_2 thin films grown on Al_2O_3(10-10) substrate and fluorine mica substrate, respectively.

In order to obtain the thermal conductivity of the VO_2 thin film through the thermal reflection curve of the film, the Thermal Analysis for Thin Films software supplied in the nanoTR system is used to analyze the curve. This simulation method uses a mirror image method. After heating the surface with a pulse, the temperature of the specimen surface changes according to the following equation:

$$T_{\mathrm{FF}}(t) = \frac{1}{b_{\mathrm{f}}\sqrt{\pi t}}\left(1 + 2\sum_{n=1}^{\infty}\gamma^n \exp\left(-n^2\frac{\tau_{\mathrm{f}}}{t}\right)\right). \quad (1)$$

Here, τ_{f} represents the characteristic time (thermal diffusion time) that describes the thermal diffusion from the surface of the thin film to the interface between the film and its substrate,

$$\gamma = (b_{\mathrm{f}} - b_{\mathrm{s}})/(b_{\mathrm{f}} + b_{\mathrm{s}}) = (1-\beta)/(1+\beta), \quad (2)$$

with b_{f} and b_{s} being the thermal effusivity of the thin film and the substrate, respectively. and $\beta = b_{\mathrm{s}}/b_{\mathrm{f}}$ representing the thermal effusivity ratio.

By using the analysis software, the thermal diffusion time τ_{f} and a dimensionless parameter γ for the thin film are determined through fitting this equation over an optimum time span with the top film used as the first layer and the substrate as the second layer. Then the thermal conductivity of the film is calculated from the thermal diffusion time according to

$$\lambda_{\mathrm{f}} = \frac{d_{\mathrm{f}}^2 \cdot \rho_{\mathrm{f}} \cdot c_{\mathrm{f}}}{\tau_{\mathrm{f}}}, \quad (3)$$

where λ_{f} is the thermal conductivity of the film, d_{f} is the thickness of the film, ρ_{f} is the density of the film, and c_{f} is the specific heat capacity of the film.

To verify the above argument, we first measure and simulate the thermal conductivities of VO_2 thin films with thickness values of 30 nm, 60 nm, and 110 nm on the Al_2O_3(10-10) and fluorine mica substrates, which are shown in Fig. S4 and Table S1 (supplementary materials). Even though the results show that the simulated thermal conductivities of all the VO_2 thin films at the metallic phase (353 K) are larger than those at the insulating phase (297 K), in consistence with that expected from the properties of VO_2, the data of 30-nm-thick and 60-nm-thick VO_2 thin films are much lower than the values of VO_2 reported in Refs. [8,10]. Furthermore, it should be noted that the thermal conductivity increases as the thickness of the VO_2 film increases. This is caused by the short heat flow diffusion time when the thickness of the VO_2 thin film is too small. Based on the calculation above, for the film with thickness below 100 nm, a picosecond laser should be utilized to improve the temperature response time.

On the other hand, because of the fast temperature response of VO_2 to infrared light, reasonable thermal conductivity value of 150-nm VO_2 thin film should be able to be measured with a nanosecond laser. We measure the thermal reflectance curves of 150-nm-thick VO_2 thin films on the Al_2O_3(10-10) substrate and the fluorine mica substrate, without an extra metal layer on their top, at 297 K and 353 K, respectively, and the curves are shown in Figs. 3(a)–3(d). The fitting results are also shown in Fig. 3. At 297 K, the simulated thermal diffusion time of the 150-nm-thick VO_2 thin films on Al_2O_3(10-10) substrate and the fluorine mica substrate are 13.19 ns and 9.97 ns, respectively. Utilizing Eq. (3) and the heat capacity per unit volume of VO_2 in Ref. [6], the simulated thermal conductivity of the 150-nm-thick VO_2 thin films on the Al_2O_3(10-10) substrate and the fluorine mica substrate are 4.86 W/mK and 6.43 W/mK, respectively. At

353 K, the thermal conductivity of the 150-nm-thick VO_2 thin films on Al_2O_3(10-10) substrate and fluorine mica substrate are 7.62 W/mK and 7.06 W/mK, respectively. While the temperature increases to 373 K, the thermal reflectance curve of the 150-nm-thick VO_2 thin film on Al_2O_3(10-10) is the same as that at 353 K as shown in Fig. S5 in the supplementary materials. In this case, the thermal conductivity of VO_2 thin film at 353 K is a stable value of metallic VO_2. It is obvious that the thermal conductivity of the VO_2 thin film on the Al_2O_3(10-10) substrate has a larger rate of change across the phase transition than that on the fluorine mica substrate. The calculated phonon thermal conductivity of metallic phase of VO_2 has a reduction resulting from the calculated phonon thermal conductivity of insulating phase of VO_2.[10] Therefore, the increase of thermal conductivity of the VO_2 thin film across MIT is due to the increase of electronic thermal conductivity. In order to explore the difference, the electrical conductivity of VO_2 thin film should be considered.

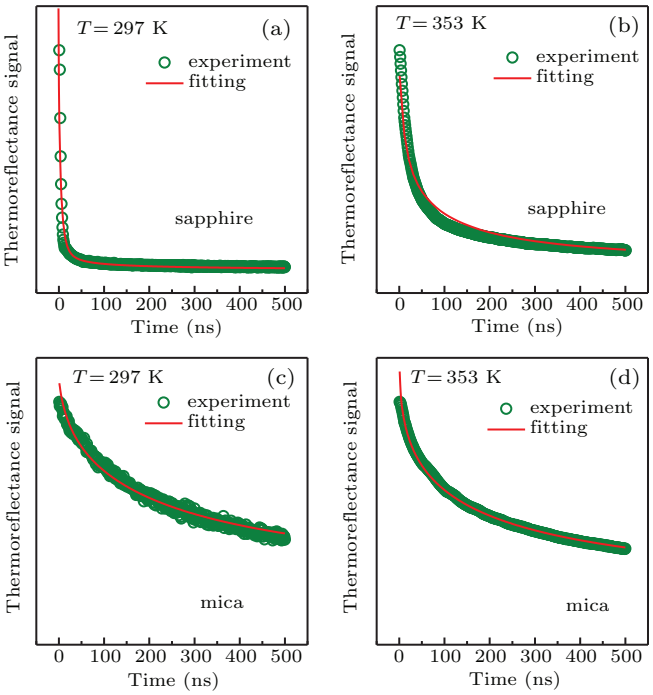


Fig. 3. Thermal reflectance curves of 150-nm-thick VO_2 thin films grown on Al_2O_3(10-10) at (a) 297 K and (b) 353 K, respectively. Thermal reflectance curves of 150-nm-thick VO_2 thin films grown on fluorine mica at (c) 297 K and (d) 353 K, respectively. Olive circles represent experimental data, and red solid lines denote fitting data.

The temperature-dependent electrical conductivities of the 150-nm-thick VO_2 thin films on different substrates are measured by four-point-probes, and the results are shown in Fig. 4. For the 150-nm-thick VO_2 film on Al_2O_3(10-10), the electrical conductivity changes from 37.6 S/m (at 297 K) to 1.44×10^6 S/m (at 353 K), while the electrical conductivity varies from 46.2 S/m (at 297 K) to 1.09×10^5 S/m (at 353 K) for the VO_2 thin film on the mica substrate. In the metallic state, the electrical conductivity of the VO_2 thin film on the sapphire substrate is an order of magnitude higher than that on the mica substrate. This phenomenon should be attributed to the crystalline quality of the films. The VO_2 thin films epitaxially grown on Al_2O_3(10-10) have better crystallinity and less defects. However, the interaction force between the fluorine mica substrate and the VO_2 film is the van der Waals force, and the XRD pattern in Fig. 2 indicates that the VO_2 thin film has only a preferred growth orientation along ⟨011⟩. Thus, the VO_2 thin film has more defects, which increases the elastic electron scattering weight.

It should be noted that the metallic phase of VO_2 is not regarded as a conventional Fermi liquid,[25,26] where the transport mode of charge and the transport mode of heat current are separated.[10] In this case, the electronic thermal conductivity of metallic VO_2 is not proportional to its electrical conductivity, which means that it does not obey the Wiedemann–Franz (WF) law. However, it has been found that disorders can recover the WF law.[11] Consequently, because VO_2 thin film has more defects than the single-crystalline VO_2 nanowires, the electronic thermal conductivity in the VO_2 thin film is related to its electrical conductivity.

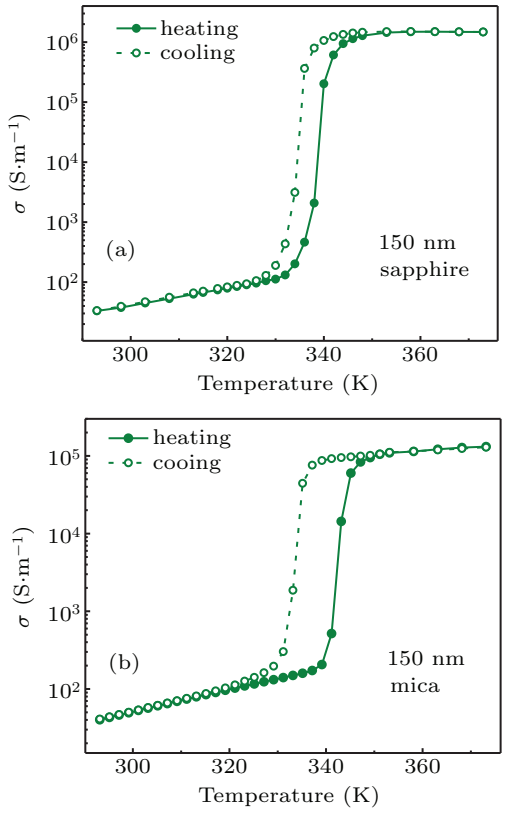


Fig. 4. Temperature-dependent electrical conductivities of 150-nm-thick VO_2 thin films grown on (a) Al_2O_3(10-10) and (b) fluorine mica, respectively.

4. Conclusions

In this work, the thermal conductivities of the VO_2 thin films on different substrates are successfully measured by TDTR without depositing any metal thermoreflectance layer. When the thickness is greater than 100 nm, the thermal con-

ductivity value is consistent with those measured by other methods. A comparison of thermal conductivity among the VO_2 thin films on different substrates shows that the thermal conductivity change rate across MIT is related to the electrical conductivity change rate, implying that the increasing elastic electron scattering weight caused by defects in the VO_2 thin film can change the electronic thermal transport mode in the metallic phase.

References

[1] Jerominek H, Picard F and Vincent D 1993 *Opt. Eng.* **32** 2092
[2] Lu C, Liang W, Gao M, Luo S N and Lin Y 2019 *IEEE Trans. Terahertz Sci. Technol.* **9** 177
[3] Zhou G, Dai P, Wu J, Jin B, Wen Q, Zhu G, Shen Z, Zhang C, Kang L, Xu W, Chen J and Wu P 2017 *Opt. Express* **25** 17322
[4] Wu C, Feng F and Xie Y 2013 *Chem. Soc. Rev.* **42** 5157
[5] Kruger B A, Joushaghani A and Poon J K S 2012 *Opt. Express* **20** 23598
[6] Zhao J X, Song J L, Zhou Y, Liu Y C and Zhou J H 2020 *Chin. Phys. Lett.* **37** 064204
[7] Kizuka H, Yagi T, Jia J, Yamashita Y, Nakamura S, Taketoshi N and Shigesato Y 2015 *Jpn. J. Appl. Phys.* **54** 053201
[8] Oh D W, Ko C, Ramanathan S and Cahill D G 2010 *Appl. Phys. Lett.* **96** 151906
[9] Dahal K, Zhang Q, He R, Mishra I K and Ren Z 2017 *J. Appl. Phys.* **121** 155103
[10] Sangwook L, Hippalgaonkar K, Yang F, Hong J, Ko C, Suh J, Liu K, Wang K, Urban J J, Zhang X, Dames C, Hartnoll S A, Delaire O and Wu J 2017 *Science* **355** 371
[11] Jin L, Zeltmann S E, Choe H S, Liu H, Allen F I, Minor A M and Wu J 2020 *Phys. Rev. B* **102** 041120
[12] Chen L, Xiang Z, Tinsman C, Asaba T, Huang Q, Zhou H and Li L 2018 *Appl. Phys. Lett.* **113** 061902
[13] Cahill D G 2004 *Rev. Sci. Instrum.* **75** 5119
[14] Taketoshi N, Baba T, Schaub E and Ono A 2003 *Rev. Sci. Instrum.* **74** 5226
[15] Capinski W S and Maris H J 1996 *Rev. Sci. Instrum.* **67** 2720
[16] Bonello B, Perrin B and Rossignol C 1998 *J. Appl. Phys.* **83** 3081
[17] Baba T, Taketoshi N and Yagi T 2011 *Jpn. J. Appl. Phys.* **50** 11RA01
[18] Piotrowski M, Franco M, Sousa V, Rodrigues J, Deepak F L, Kakefuda Y, Kawamoto N, Baba T, Owens-Baird B, Alpuim P, Kovnir K, Mori T and Kolen'ko Y V 2018 *J. Phys. Chem. C* **122** 27127
[19] Kakefuda Y, Yubuta K, Shishido T, Yoshikawa A, Okada S, Ogino H, Kawamoto N, Baba T and Mori T 2017 *APL Mater.* **5** 126103
[20] Liu K, Zhao J, Sun H, Guo H, Dai B and Zhu J 2019 *Chin. Phys. B* **28** 060701
[21] Zhang Y Y, Cheng R, Ni D, Tian M, Lu J W and Zhao Y 2019 *Chin. Phys. B* **28** 078105
[22] Jia Q X, McCleskey T M, Burrell A K, Lin Y, Collis G E, Wang H, Li A D Q and Foltyn S R 2004 *Nat. Mater.* **3** 529
[23] Ji Y D, Pan T S, Bi Z, Liang W Z, Zhang Y, Zeng H Z, Wen Q Y, Zhang H W, Chen C L, Jia Q X and Lin Y 2012 *Appl. Phys. Lett.* **101**
[24] Liang W, Gao M, Lu C, Zhang Z, Chan C H, Zhuge L, Dai J, Yang H, Chen C, Park B H, Jia Q and Lin Y 2018 *ACS Appl. Mater. Interfaces* **10** 8341
[25] Allen P B, Wentzcovitch R M, Schulz W W and Canfield P C 1993 *Phys. Rev. B* **48** 4359
[26] Qazilbash M M, Burch K S, Whisler D, Shrekenhamer D, Chae B G, Kim H T and Basov D N 2006 *Phys. Rev. B* **74** 205118